International Journal of Heat and Mass Transfer 52 (2009) 4236–4243

Contents lists available at ScienceDirect

International Journal of Heat and Mass Transfer

journal homepage: www.elsevier.com/locate/ijhmt

The effect of chemical reaction on the mixing flow between aqueous solutions of acetic acid and ammonia

Satoshi Someya [a,b,*], Satoshi Yoshida [a], Takahide Tabata [c], Koji Okamoto [a]

[a] Graduate School of Frontier Science, The University of Tokyo, Kankyo-Building 221, Kashiwanoha 5-1-5, Kashiwa, Chiba 277-85563, Japan
[b] National Institute of Advanced Industrial Science and Technology, 1-2-1 Namiki, Tsukuba, Ibaraki 305-8564, Japan
[c] Kagoshima National College of Technology, 1460-1 Shinko, Hayato, Kirishima, Kagoshima 899-5193, Japan

ARTICLE INFO

Article history:
Received 1 October 2008
Received in revised form 28 January 2009
Accepted 8 April 2009
Available online 19 May 2009

Keywords:
Mixing
Flow visualization
Chemical reaction
Jet

ABSTRACT

The basic characteristics of the reacting mixing flow of two streams were investigated. The reaction between aqueous solutions of ammonia and acetic acid, which produces ammonium acetate, was investigated in terms of the effect on the fluid–fluid interface of the mixing flow relative to fluids that did not react. The reaction between these solutions was negligibly exothermic, and there were minimal differences in density. The velocity field in the reacting mixing flow was quantitatively measured using high-speed time-resolved particle image velocimetry (PIV) and the behavior of the mixing flow was qualitatively investigated using laser-induced fluorescence (LIF). The jet width, the velocity field, the kinetic energy and the turbulent intensities are qualitatively estimated and discussed. It was found that the chemical reaction resulted in the suppression of the mixing flow.

1. Introduction

Many industrial processes involve chemical reaction under turbulent flow. Understanding the effect of the turbulence structure on the chemical reaction kinetics is still an open question, one that is important for the development of models based on flow characteristics. A planar jet exhibits a typical shear flow involving intensive interaction between neighboring streams and having vortical characteristics typical of turbulent flows. Experimental studies offer an intuitive and direct method to clarify the structures of turbulent jets and numerous studies have been performed in this area [1–8].

Similar to a non-reacting plume, a reacting flow can undergo a transition from laminar to turbulent flow following a vortex breakdown in the transitional region. Vortex dynamics are expected to be crucial for describing these near-field phenomena and the transition from jet-like to plume-like behavior in the far field. Kawanabe et al. [9] measured the velocity distribution in a methane jet flame and a nitrogen jet. They showed that the time-averaged velocity in the flame was larger than that in the non-reacting jet due to buoyancy. They also concluded that the turbulence intensity in the flame becomes larger due to the local volume expansion arising from combustion. Ito et al. [4], Nagata et al. [5], Komori et al. [6,7] and Bennani et al. [8] have investigated the effects of flow on chemical reactions and turbulent mixing. They carried out experiments in stable/unstable density stratified flows and discussed the results in terms of counter-gradient heat transfer. Hong et al. [10] reported that a chemical reaction affected the mixing of a horizontal liquid round jet.

In this report, the basic characteristics of a reacting mixing flow are investigated. The reaction between an ammonia solution and an acetic acid solution was studied in terms of its effect on the fluid–fluid interface of the mixing flow. The reaction has a negligible reaction heat. The two mixing solutions are very similar in terms of their densities and their other thermo-physical properties such as viscosity. However, it is expected that very small changes in the thermo-physical properties of the solutions arising from chemical reaction would affect the mixing flow and the interfacial stability. Experiments were performed in two different apparatuses. First, the mixing flow of an upward round jet and an upward ambient flow was studied. Second, the interfacial instability of a parallel flow in a rectangular tank was investigated in order to suppress small buoyancy effects.

2. Experiments and discussion

2.1. Experiments in a round-jet system

A schematic of the experimental setup is shown in Fig. 1. The base of the acrylic main-tank was 150 × 150 mm^2 and the height was 1500 mm. In order to maintain a uniform ambient flow, two

* Corresponding author. Address: Graduate School of Frontier Science, The University of Tokyo, Kankyo-Building 221, Kashiwanoha 5-1-5, Kashiwa, Chiba 277-85563, Japan. Tel.: +81 4 7136 5872; fax: +81 4 7136 4603.
E-mail address: some@k.u-tokyo.ac.jp (S. Someya).

0017-9310/$ - see front matter © 2009 Elsevier Ltd. All rights reserved.
doi:10.1016/j.ijheatmasstransfer.2009.04.005

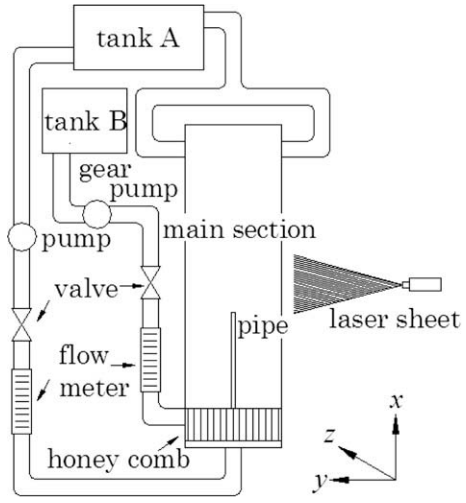

Fig. 1. Schematic of experimental setup.

honeycombs made of aluminum were installed in the lower part of the tank. A copper tube 1 mm in inner diameter and 2 mm in outer diameter was installed at the center of the flow channel and extended 100 mm from the honeycomb. The total length of the copper nozzle was 290 mm. The coordinate origin for the experiments was the center of the edge of the inlet nozzle.

The jet flow and ambient flow were supplied from the head tanks and did not have any periodic fluctuations. The velocity of the ambient flow was initially kept constant at 23.6 mm/s. The working fluids overflowed uniformly in the left and right directions at the top of the main tank. The inlet velocity, Uin, of the upward jet from the copper nozzle was varied from 211 to 636 mm/s discretely (212, 255, 297, 340, 382, 531 and 636 mm/s).

The working fluids used in the experiments are summarized in Table 1; a chemical reaction occurred only in case D. The Reynolds number of the jet flow was varied from 210 to 630 and that of the ambient flow was 2220. The temperature of the working fluids was kept constant at 25–26 °C. The temperature was also monitored downstream, and a temperature change was not detected in any of the experiments. The reaction rate constant, k, is 10^8 $m^3/(mol\ s)$ [4–7,10,11] and the reaction heat is 13.8 kcal/mol [10]. The concentration of each aqueous solution, pH and density are summarized in Table. 1. The density of each solution was 997.1 (acetic acid), 997.0 (ammonia), 997.0 (water) kg/m^3. The differences in the density (0.01%) and the heat of reaction in case D (about 6.5×10^{-2} cal/ml) were small. In the experiments, as shown in Fig. 1, the mixed solution was returned to the buffer tank A. The pH was monitored to ensure that there was no change in pH over the short duration of each experiment. When a small change in pH (±0.02) was detected in tank A, the solution was freshly prepared.

At first, in order to qualitatively investigate the mixing behavior of the flow, simple experiments were done using laser-induced fluorescence (LIF). The LIF measurements were carried out using an Ar-ion laser (4 W) and a CMOS camera (Basler A602f, 656×491 pixel, 8-bit gray, 100 fps). The exposure time was set to 1.5 ms. A fluorescent dye (rhodamine 6G) was premixed into the jet flow. The diffusion of the dye showed the mixing behavior. The concentration of the dye was kept constant at 1.0×10^{-6} mol/L. For the LIF measurements, an optical filter (Nikon O56) that only transmitted light at wavelengths greater than 560 nm was attached to the camera in order to block light due to reflection of the incident and scattered light.

The jet behavior in cases A–D could be successfully visualized by the simple LIF measurement, with the diffusion of the fluorescent dye qualitatively showing the mixing behavior. Fig. 2 shows superimposed images of five sequential LIF images captured at an interval of 1/100 s. The grey scale intensity of the superimposed images only shows the qualitative jet behavior (width), while the grey scale intensity of each image at a certain moment indicates the instantaneous concentration of the jet fluid (concentration of dye). The inlet velocity, Uin, was set at 297 or 340 mm/s and the inner diameter of the inlet nozzle, d, was 1 mm (Fig. 2). These images show the flow and the behavior of the jet diffusion 10–60 mm downstream of the inlet nozzle. At Uin values less than 255 mm/s, independently of the working fluids, the injected free round jet flowed downstream with a spiral rotation.

In case A, there was no difference in the thermo-physical properties of the ambient flow and the jet and there was no chemical reaction. Here, the jet width became large with increasing jet inlet velocity. In cases B and C, the properties of the solutions were different between the ambient flow and the jet and although there was no chemical reaction, there was mass transfer in the mixing region. Nonetheless, the behavior of the jet flow in cases B and C was similar to that in case A and only minor differences were observed. In cases B and C, the jet width upstream (at $x/d = 10$) remained narrow at the velocity Uin = 297. Overall, among cases A–C, the jet spread downstream was similar and there were minimal differences in the jet width and the development of turbulence. The jet width became large with increasing jet inlet velocity. Here, the diffusion of the dissolved substance did not significantly affect the development of turbulence. On the other hand, in case D, where a chemical reaction occurred, the mixing of the jet and the ambient fluid was suppressed and hardly any turbulence was observed, even downstream. The jet width did not increase, even downstream, or when the inlet velocity, Uin, was increased from 297 to 340 mm/s. The suppression of mixing was particularly remarkable in this range. At Uin $\leqslant$ 297 mm/s or Uin $\geqslant$ 340 mm/s, the development of turbulence was not significantly different among cases A–D.

The differences observed between case D and the other cases are considered to result from the chemical reaction occurring at the interface between the ambient fluid and the jet. All species should be passive. The differences in density and the reaction heat are not very large. We were unable to estimate the viscosities of the solutions due to their low concentrations; however, any difference between them is expected to be small. This key parameter is still unknown but mixing is only suppressed in case D, in which there is a chemical reaction.

At Uin $\geqslant$ 382 mm/s, the jet width increased at values of x/d between 20 and 30, and it did not develop much further downstream ($x/d > 30$). At greater Uin, the mixing flow that occurs with the

Table 1
Working fluids.

Case	Jet	Ambient flow
A	Water (pH 6.66)	Water (pH 6.56)
B	Acetic acid (pH 3.64, 3.14×10^{-3} mol/l, 997.1 kg/m^3)	Water (pH 6.62)
C	Ammonia (pH 10.40, 3.78×10^{-3} mol/l, 997.0 kg/m^3)	Water (pH 6.68)
D	Acetic acid (pH 3.55, 4.70×10^{-3} mol/l, 997.1 kg/m^3)	Ammonia (pH 10.52, 6.46×10^{-3} mol/l, 997.0 kg/m^3)

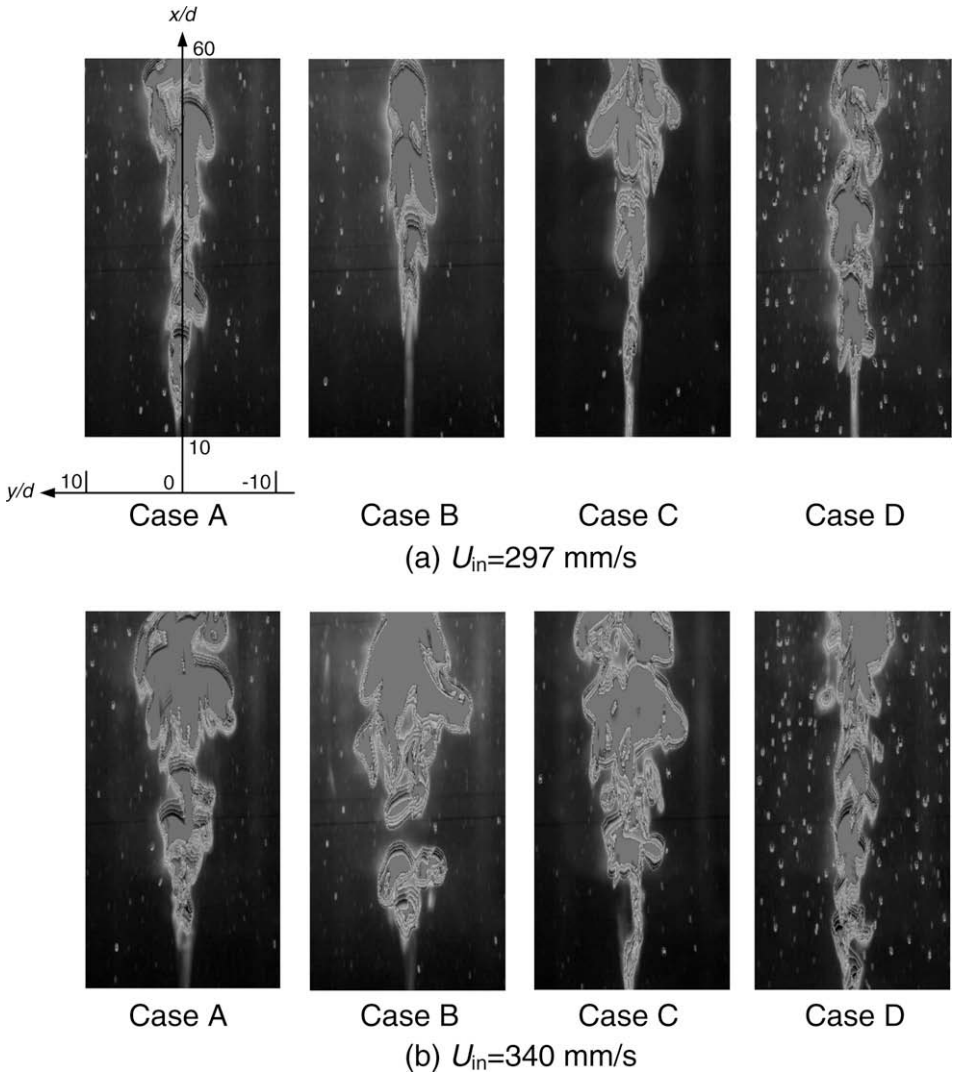

Fig. 2. Superposition of five sequential images taken of the injected jet flow.

larger kinetic energy might be dominated by turbulent mixing, and the chemical reaction could not influence the flow.

The results obtained from the superimposed images were very useful qualitatively. However, more quantitative data is necessary to better understand the phenomenon. As such, the velocity in the mixing region was measured using particle image velocimetry (PIV). The PIV measurements were carried out using a double-pulse laser (YAG, 532 nm, 30 Hz) and a frame straddling technique with a CCD camera ($10^3 \times 10^3$ pixel, 8 bit). The spatial resolution was 29.4×10^{-3} mm/pixel. As a tracer for the PIV measurements, particles of nylon-12 (Orgasol 202 ES3 NAT3, average diameter: 30 μm) were premixed into the ambient fluid. The particles were seeded into the ambient flow only. The technique was accurate enough to measure the flow at the mixing region, though the measurement accuracy was lower within the jet as compared to the outside, especially upstream.

Fig. 3 shows the averaged velocity distribution at 6.67 s, measured downstream (x/d = 40, 40 mm from the inlet nozzle) at various inlet velocities (255, 297, 340 mm/s). In cases A, B and C, the maximum velocity at the center of the jet decreased with increasing jet inlet velocity, due to the promotion of jet diffusion arising from the development of turbulence at higher inlet velocities. There were small differences of thermo-physical properties between solutions in cases B and C, however, the velocity distribution shown in Fig. 3 were similar in cases A, B and C. The effect of the small differences of thermo-physical properties could not be observed.

In case D, the maximum velocity at the center also decreased with an increase in the inlet velocity from 255 to 297 mm/s. However, the maximum velocity at the center remained the same when the inlet velocity was further increased to 340 mm/s. Indeed, the velocity distribution observed at inlet velocities of 297 and 340 mm/s was nearly identical. At Uin = 255, the velocity distribution observed for case D was identical to those in cases A–C, that is, there was no discernable effect of the initial differences in density and reaction heat for the low Re number case.

In order to further investigate this phenomenon, the jet width was estimated from the velocity distribution. Fig. 4 shows the jet width at a certain distance from the inlet, x/d, for cases A–D at an inlet velocity of 340 mm/s. The jet width (2b) represents the distance from the center of the jet to the point where the relative velocity becomes 10% of the maximum value. It was difficult to estimate the jet width at x/d smaller than 10 due to a lack of tracer particles in this region.

In cases A, B and C, the jet spread gradually downstream and there were no significant differences among these cases. However, the rate of increase in the jet width was obviously much smaller in case D.

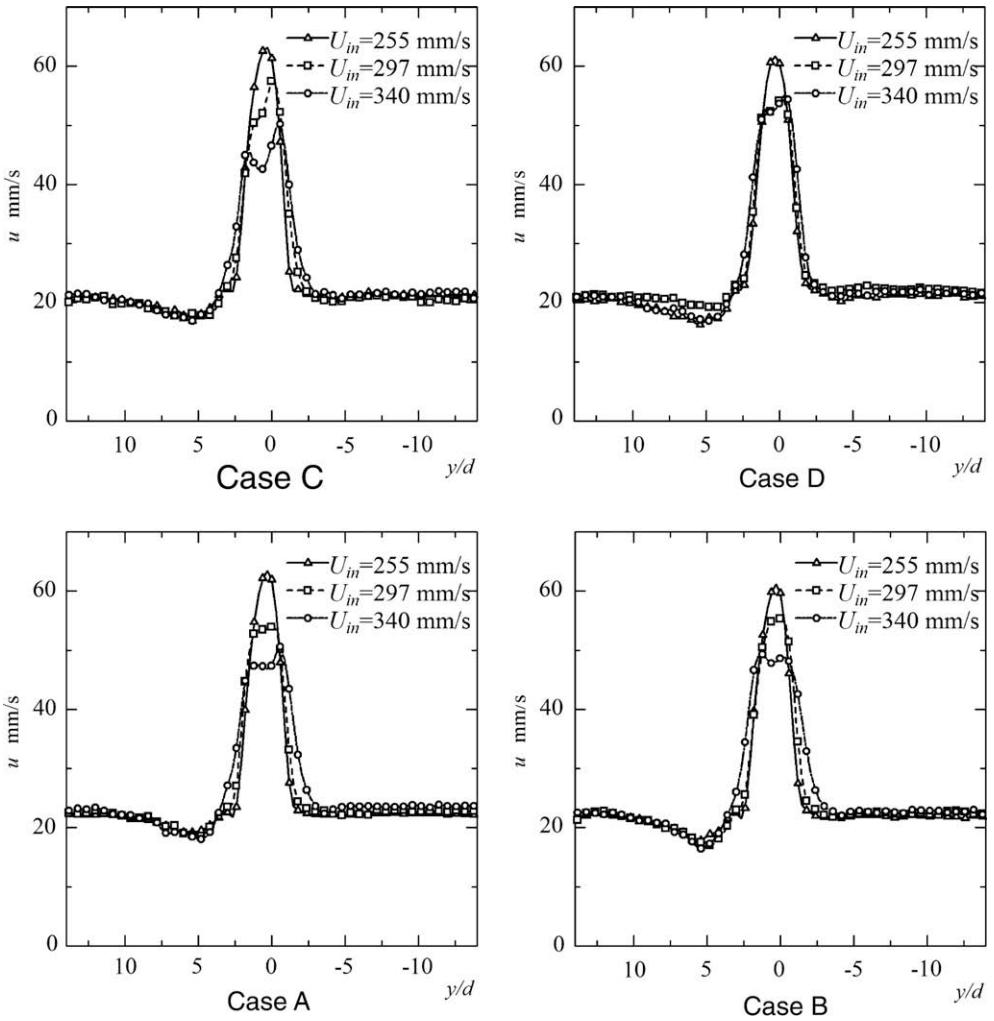

Fig. 3. The distribution of the vertical velocity at Uin = 255–340 mm/s.

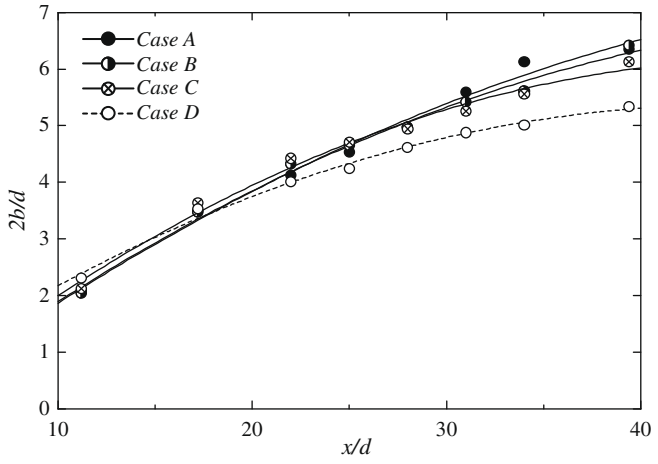

Fig. 4. The jet width downstream at Uin = 340 mm/s.

In the mixing region in case D, acetic acid reacts with the ammonium solution, giving ammonium acetate and pure water as products. These products might alter the viscosity and density of the working fluid. In addition, the reaction heat should affect the density of the working fluid. These changes can affect the flow field. We cannot be sure at this stage which property affects the mixing flow. However, it is a fact that the mixing due to the development of turbulence was suppressed in case D presumably as a result of chemical reaction.

Figs. 3 and 4 summarize the vertical velocities. The differences in jet width are remarkable at a vertical position of $x/d = 40$ and an inlet velocity of 340 mm/s. By visual inspection of the images, the mixing region at $x/d = 40$ was estimated to be around $y/d = 6–8$. From this estimate, the kinetic energy of the jet flow was calculated for cases A and D. Fig. 5 shows the kinetic energy normalized by the square of the inlet velocity at $x/d = 40$ for inlet velocities of 297, 340 and 382 mm/s, for the region $y/d = 5–9$.

In case A, the kinetic energy increased with an increase in the inlet velocity from 297 to 340 mm/s, both outside ($y/d = 6–8$) and inside the mixing region ($y/d = 5–6$).

On the other hand, in case D, the kinetic energy, as calculated from the two-dimensional velocity distribution did not change with an increase in inlet velocity from 297 to 340 mm/s in the range $y/d = 5–9$.

At an inlet velocity of 382 mm/s, there were no differences in the kinetic energy distributions of cases A and D. It is thought that the kinetic energy of the jet flow at this velocity becomes so large that the chemical reaction and the ripple effects of the reaction no longer affect the flow.

In order to investigate the suppression of turbulence due to chemical reaction in more detail, the velocity distribution and the jet width at $x/d = 40$ were monitored at various velocities

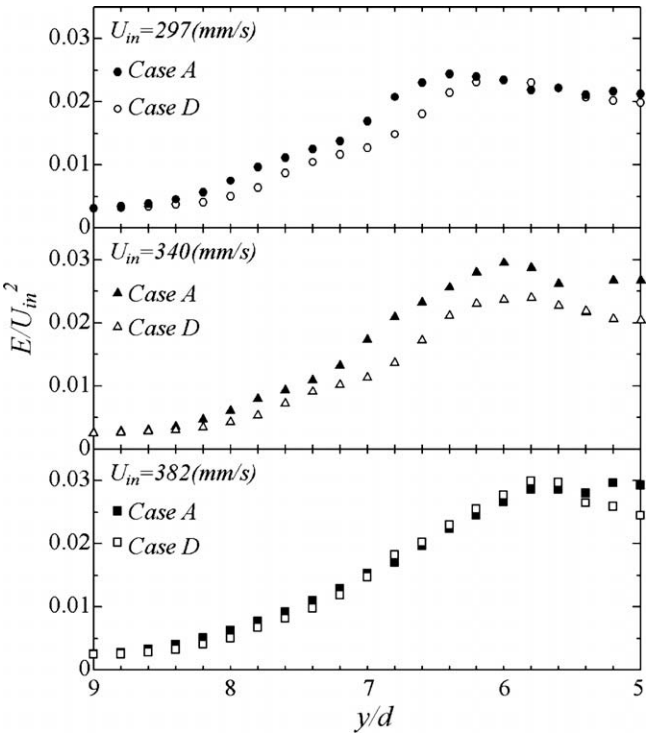

Fig. 5. Distribution of Kinetic Energy (x/d = 40).

(0.0, 4.72, 14.1, 23.6 mm/s) of the ambient flow for cases A and D. Fig. 6 shows the velocity distribution at x/d = 40. The jet inlet velocity was kept constant at 340 mm/s (Re = 335).

In case A, where there was no chemical reaction, the maximum velocity at the center (y/d = 0) increased with increasing velocity of the ambient flow. Both the relative velocity at the center and the jet width increased with decreasing velocity of the ambient flow, at least in the range of experimental conditions shown in Fig. 6. The relative velocity distribution and the jet width were hardly affected by the velocity of the ambient flow.

In case D, where there was a chemical reaction, the maximum velocity at the center (y/d = 0) was not affected by the velocity of the ambient flow. It is thought that the reaction products forming at the interface might affect the viscosity of the working fluid and consequently the shear flow. Any change in thermo-physical properties such as interfacial tension and viscosity would also likely affect the slip flow.

Fig. 7 shows the jet width at different velocities of the ambient flow. The jet widths in case D, shown by dotted lines, were smaller than those in case A, over all conditions. The relative inlet velocities in Figs. 6 and 7, (U_{in}–$U_{ambient}$), were 316.4–340 mm/s. Over this range, the difference in jet width between cases A and D increased with the difference in relative velocity between them. The rate of change in the jet width was larger without the ambient flow ($U_{ambient}$ = 0). In case D, the ambient flow supplies chemical species to the interface and may also promote the reaction.

2.2. Experiments with a parallel shear flow system

The exact cause of the suppression of mixing in the case where a chemical reaction is occurring remains to be clarified. A more detailed understanding of the phenomenon is needed before an exact mechanism can be proposed at this preliminary stage. In this paper, we aim to initially report the details of the phenomenon. To further investigate, we also performed experiments using high speed time-resolved PIV and a rectangular channel tank system, in which two fluids were injected parallel (not stratified flow) to minimize any effect of a difference in densities (buoyancy), which is less significant in this apparatus than in the round-jet system.

Fig. 8 shows a schematic of the experimental apparatus based on a rectangular channel and Fig. 9 gives the dimensions of the rectangular channel. Different aqueous solutions were circulated and measured using the LIF and PIV techniques. Each fluid was pumped and passed through a flow meter. Honeycombs assisted the creation of a uniform and steady inlet flow condition. The rectangular channel was made of acrylic resin. The channel was 800 mm long and had 2-mm-thick vertical plates (2 mm (=2T)) positioned along the center axis of the tank at each end with a 150 mm gap in the middle for mixing. The width of the channels on either side of the vertical plates was 30 mm and that in the mixing region was 62 mm. The aqueous solutions could only mix in this region. The channels were positioned horizontally such that the acceleration due to gravity was directed perpendicular to the page in the schematic (Fig. 9). In this system, the initial density difference hardly affects the mixing. After mixing, the partly neutralized aqueous solution is returned to the two tanks and recirculated. The pH of the aqueous solution was monitored to ensure there is no change in pH over the short duration of each experiment. Two different pairs of liquids, given as cases A and B

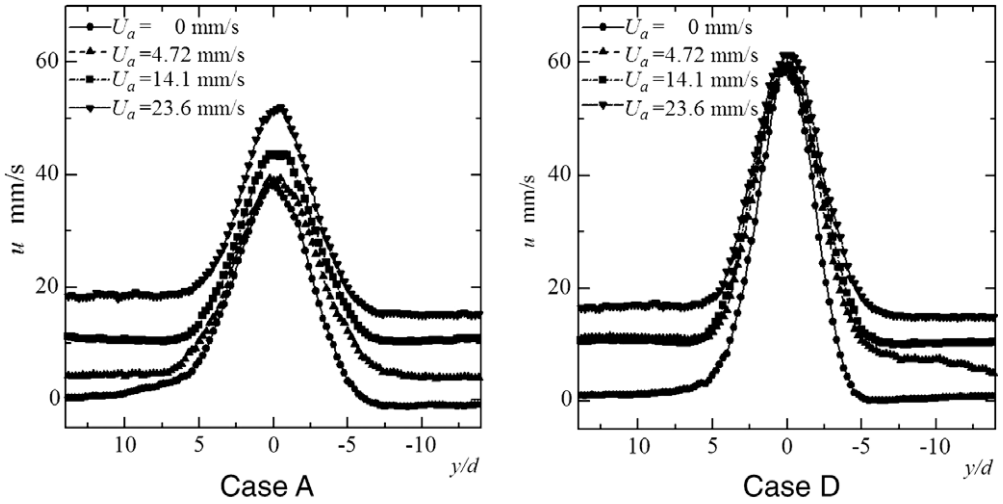

Fig. 6. The vertical velocity distributions at different velocities of ambient flow.

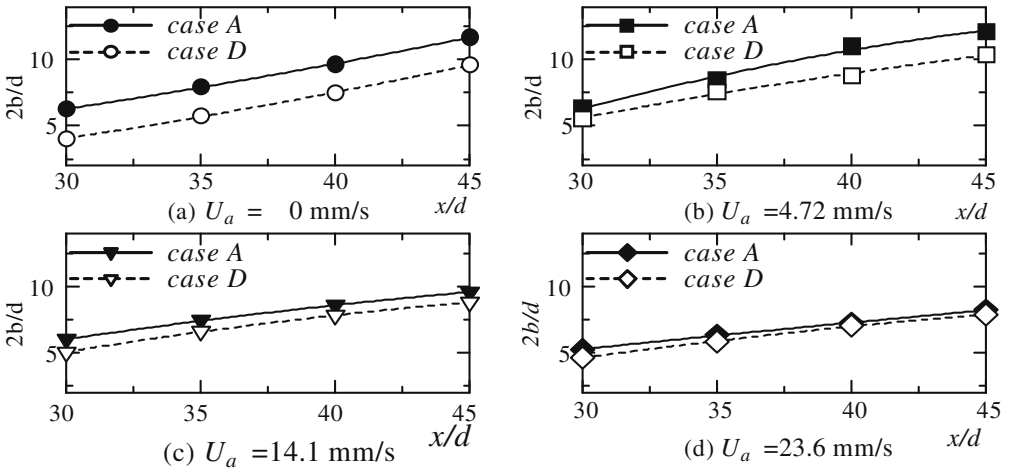

Fig. 7. The jet width at different velocities of ambient flow.

in Table 2, were investigated: one with a chemical reaction and the other without.

LIF or PIV measurements were carried out for the experiments in the rectangular channel. Again, the fluorescent dye (rhodamine 6G) was premixed into the fluid in channel 1 only in order to qualitatively investigate the mixing behavior of the flows. The dye concentration was kept constant at 1.0×10^{-6} mol/L. The optical systems and the seeding particles used in the PIV measurement were the same as those in the experiments with the round jet. However, a different laser and camera were used. A high-speed double-pulse laser (Nd:YLF) and a high-speed camera were used. The mixing flow was investigated over the range of Re = 1250–3100 (4.2–10.3 cm/s of mean velocities).

Fig. 10 shows the mixing behavior of the fluorescent dye. In this figure, the origin is the upstream open edge of the plate (the starting point of the mixing area). The *x*- and *y*-directions are as indicated; here, T indicates half the width of the partition plate.

At Re = 1250, the fluid from each channel did not mix much, even downstream, for both cases A and B. The wavelength at the interface was smaller for case A, where there was no chemical reaction. At Re numbers above 1900, the mixing flow was obviously suppressed (Fig. 10(f)–(h)) for case B in which there was a chemical reaction. The patterns in Fig. 10(b)–(d) appear very complicated.

In order to investigate the mixing flow quantitatively, the velocity distribution was measured using high-speed time-resolved PIV, known as dynamic PIV (DPIV). The frequency of the DPIV in our experiments was 1000 Hz and the flame straddling technique was not applied.

The time series data obtained for the velocity component are summarized in Fig. 11. No dominant frequency was observed in the data. However, it was clarified that the frequency of the velocity fluctuation was lower in case B than that in case A. Fig. 10(c) and (g) indicated a similar result. The wavelength at the interface

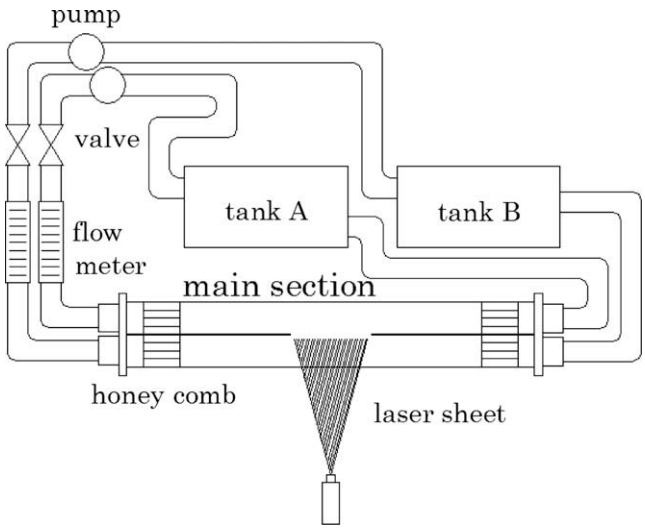

Fig. 8. Schematic of the rectangular tank system.

Table 2
Liquid pairs in experiments in the rectangular tank.

Case	Channel 1	Channel 2
A	Water (pH 6.85)	Water (pH 6.85)
B	Acetic acid (pH 4.03, 5.8×10^{-4} mol/l, 997.1 kg/m^3)	Ammonia (pH 9.84, 3.4×10^{-4}mol/l, 997.0 kg/m^3)

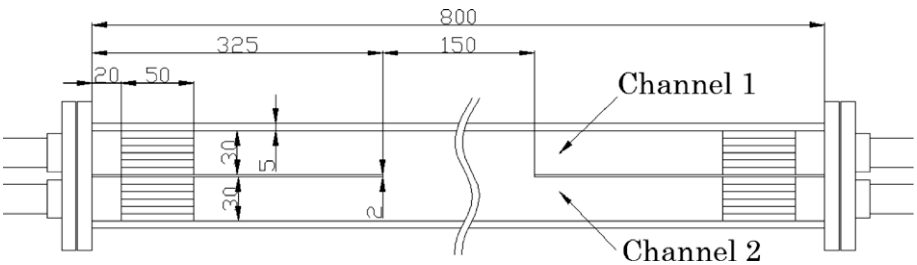

Fig. 9. Dimensions of the main tank.

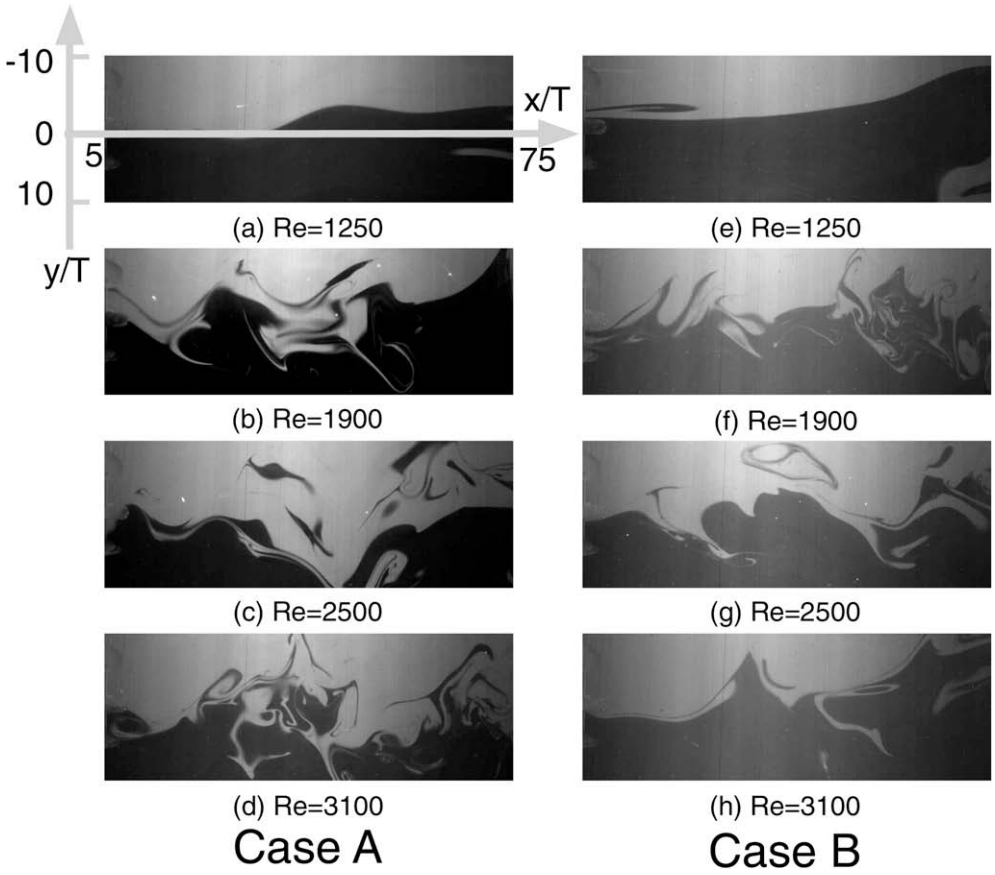

Fig. 10. Freeze-frame images of the mixing region.

was smaller in case A. The frequency of the velocity fluctuation was suppressed as a result of the chemical reaction.

Figs. 12 and 13 show the kinetic energy normalized by the square of the average inlet velocity along the x-axis at $y/T = 0$ for the cases with Re numbers of 2500 and 3100, respectively. As shown in Fig. 12, at x/T less than 32, the kinetic energy at $y/T = 0$ was smaller in the case where chemical reaction occurred than in the case where it did not. The energy values of the two cases coincided at x/T values of around 32–36.

On the other hand, in Fig. 13, the energy values of the two cases at Re = 3100 were different at x/T values less than 22 but coincided with each other at x/T values above 22. In this case (Re = 3100), the value of the kinetic energy became large and the effect of the kinetic energy on the flow field also became large. As such, it is thought that any effect of the small changes in thermo-physical properties of the solutions due to chemical reaction on the flow was relatively small in comparison to that observed under the condition with a smaller Re value (Re = 2500).

The results obtained in the rectangular channel experiment support those obtained in the round-jet system. In a certain velocity range, both systems show suppressed mixing in the case where there is a chemical reaction. The mixing due to the development of turbulence was suppressed in the case where there was a chemical reaction, presumably as a result of small changes in the viscosity distribution. However, the exact cause of the phenomena remains to be clarified. In this paper, we first report the details of the observed phenomenon. The experiments presented in this paper show that chemical reaction greatly affects the mixing flow of

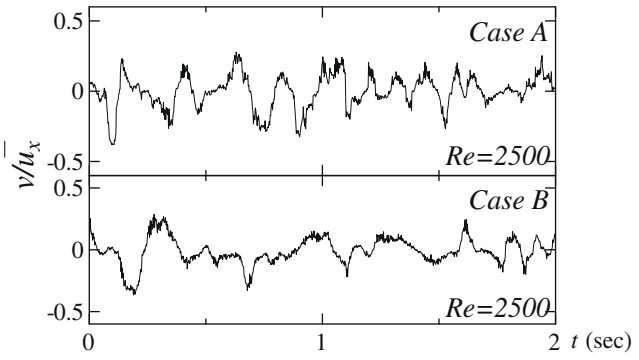

Fig. 11. Time series data of the velocity component (y-direction) at $x/T = 30$, $y/T = 0$.

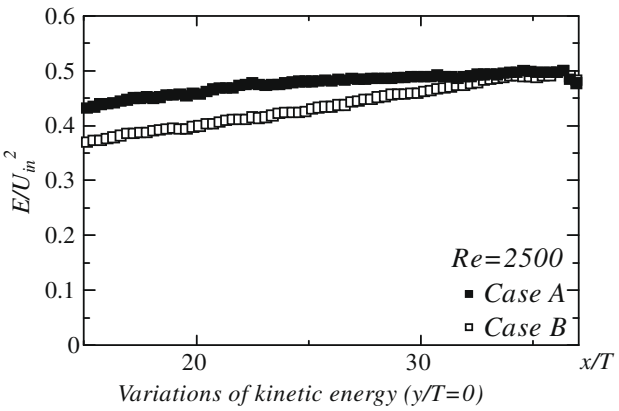

Fig. 12. The kinetic energy distribution at $y/T = 0$ (Re = 2500).

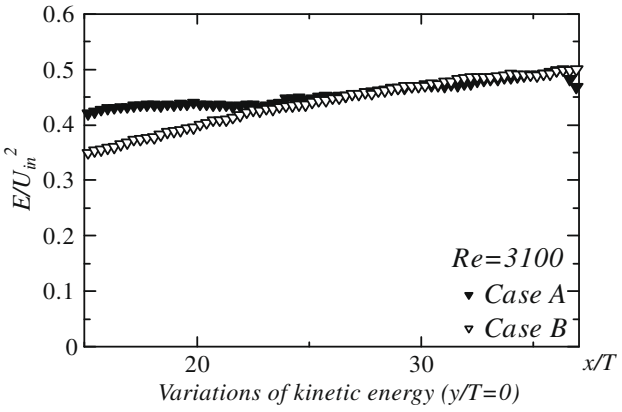

Fig. 13. The kinetic energy distribution at $y/T = 0$ (Re = 3100).

two mixing streams and suppresses the development of turbulence.

3. Conclusions

The effect of a chemical reaction on the mixing flow and the development of turbulence were investigated by dynamic PIV and LIF techniques. Experiments were carried out in two different systems, a round-jet system and a parallel shear flow system. It was found that, over a certain range of Re numbers, mixing and the development of turbulence were remarkably suppressed in the case where there was a chemical reaction. The jet width and kinetic energy distribution quantitatively supported the results. A physical mechanism of the phenomenon has yet to be clarified but the present investigation provides important details on the general characteristics of the phenomenon.

References

[1] L. Muniz, M.G. Mungal, Effects of heat release and buoyancy on flow structure and entrainment in turbulent nonpremixed flames, Combust. Flame 126 (2001) 1402–1420.
[2] W. Zhao, S. Frankel, Numerical simulations of sound radiated from an axisymmetric premixed reacting jet, Phys. Fluids 13 (9) (2001) 2671–2681.
[3] T.P. Jenkins, I.M. Kennedy, Probability density functions of product concentration in a turbulent reacting coflow jet of NH_3 and HCl, Phys. Fluids 12 (11) (2000) 3050–3059.
[4] Y. Ito, K. Nagata, S. Komori, The effects of high-frequency ultrasound on turbulent liquid mixing with a rapid chemical reaction, Phys. Fluids 14 (12) (2002) 4362–4371.
[5] K. Nagata, S. Komori, The effects of unstable stratification and mean shear on the chemical reaction in grid turbulence, J. Fluid Mech. 408 (2000) 39–52.
[6] S. Komori, T. Kanzaki, Y. Murakami, Simultaneous measurements of instantaneous concentrations of two reacting species in a turbulent flow with a rapid reaction, Phys. Fluids A3 (4) (1991) 507–510.
[7] S. Komori, K. Nagata, T. Kanzaki, Y. Murakami, Measurements of mass flux in a turbulent liquid flow with a chemical reaction, AIChE J. 39 (10) (1993) 1611–1620.
[8] A. Bennani, J.N. Gence, J. Mathieu, The influence of a grid-generated turbulence on the development of chemical reactions, AIChE J. 31 (7) (1985) 1157–11166.
[9] H. Kawanabe, K. Kawasaki, M. Shioji, Gas-flow measurements in a jet flame using cross-correlation of high-speed-particle images, Measur. Sci. Technol. 11 (2000) 627–632.
[10] S.D. Hong, K. Okamoto, H.J. Kim, Y. Sugii, H. Madarame, Chemically reacting liquid round jet, J. Visual. 6 (3) (2003) 225–234.
[11] K. Nagata, S. Komori, Effects of unstable thermal stratification and mean shear on chemical reaction and turbulent mixing in grid-generated turbulence, Trans. Jpn. Soc. Mech. Eng. B 63 (612) (1997) 274–281.